Electrochemistry Communications 57 (2015) 43–47

Contents lists available at ScienceDirect

Electrochemistry Communications

journal homepage: www.elsevier.com/locate/elecom

Atomic layer deposition derived amorphous TiO_2 thin film decorating graphene nanosheets with superior rate capability

Minsi Li [a], Xifei Li [b,*], Weihan Li [a], Xiangbo Meng [c], Yan Yu [a], Xueliang Sun [c,b]

[a] Key Laboratory of Materials for Energy Conversion, Chinese Academy of Sciences, Department of Materials Science and Engineering, University of Science and Technology of China, Anhui, Hefei 230026, PR China
[b] Energy & Materials Engineering Centre, College of Physics and Materials Science, Tianjin Normal University, Tianjin 300387, PR China
[c] Nanomaterials and Energy Lab, Department of Mechanical and Materials Engineering, Western University, London, Ontario N6A 5B9, Canada

ARTICLE INFO

Article history:
Received 7 May 2015
Received in revised form 12 May 2015
Accepted 12 May 2015
Available online 21 May 2015

Keywords:
Graphene nanosheets
TiO_2 anode
Cycling performance
Rate capability
Atomic layer deposition

ABSTRACT

Composites consisting of graphene nanosheets (GNSs) decorated with amorphous TiO_2 thin films were synthesized by an atomic layer deposition (ALD) technique. It was revealed that the TiO_2 thin films were uniformly deposited onto the worm-like GNSs. When used as anode materials in lithium ion batteries (LIBs), the TiO_2–GNS composites deliver a stable capacity of ~140 mAh g^{-1} after 100 cycles at a specific current of 100 mA g^{-1} as well as superior rate capability, accounting for a sustainable 95 mAh g^{-1} capacity at a specific current of 1200 mA g^{-1}. It is believed that the remarkable electrochemical performance lied in the unique features of the composites, i.e., the amorphous nature of the TiO_2 films and the large surface area of GNSs. The former rendered short Li^+ diffusion pathways in TiO_2 thin film, while the latter offered excellent electronic conductivity as well as a large intimate contact area between the electrolyte and TiO_2. This work laid a venue for designing new electrodes for high-performance LIBs.

1. Introduction

The TiO_2 anode features its higher insertion/extraction voltage, which can partly prevent it from side reactions at the interface between anode materials and electrolytes, and increase safety and cyclability. However, some researchers reported that solid electrolyte interphase (SEI) layer formation still occurs due to high surface area and electrocatalytic properties of TiO_2 [1–3]. Poor electron transport and slow Li-ion diffusion of TiO_2 made it unfeasible working at high rates [4–6]. To circumvent these issues, various strategies have been proposed, such as morphology control [7,8], single-crystalline creation [9], and N doping [10], to aim at enhancing kinetics of the lithium insertion/extraction processes for improved TiO_2 performance. Some approaches have been investigated to improve the electron transport of TiO_2, such as the introduction of conductive matrix [11], and conductive coating [12]. The graphene nanosheets (GNSs) were one of the most promising conductive matrices, due to its excellent electronic conductivity and mechanical properties [13]. Moreover, the three-dimension (3D) GNSs accommodate the strain caused by volume change during charge/discharge processes, and provide high specific surface areas for better contact between electrode materials and electrolytes, and thereby facilitated Li-ion transport [14,15].

Recently, it has been reported that atomic layer deposition (ALD) is a very promising strategy for the design of nanostructures for numerous applications, such as energy conversion and storage, microelectronics, sensing, originating from the advantages of depositing uniform thin films on substrates and tuning the size and thickness of target materials at the atomic scale [16,17]. So far, ALD was applied to decorate the surface of LIB electrode materials to improve electrochemical performance; in particular, this advanced technique shows a strong ability to directly create novel nanostructure materials with increased LIB performance [18,19].

Herein, we report the synthesis of nanocomposites consisting of GNSs decorated with amorphous TiO_2 thin films by ALD. Beneficial from deposition of TiO_2 at the atomic scale via ALD, the TiO_2 thin films were uniformly deposited on the GNS surface. The resultant nanocomposites were studied as anode for LIBs.

2. Experimental

GNSs were synthesized as described by our previous paper [20,21]. The amorphous TiO_2–GNS nanocomposites were synthesized in an ALD reactor (Savannah 100, Cambridge Nanotechnology Inc., USA) under 0.4 Torr at 100 °C. Titanium tetraisopropoxide (TTIP, 98%, Sigma-Aldrich) and deionized H_2O in two cylinders were used as the titanium and oxygen source, respectively. Nitrogen gas was used as the carrier gas with a flow rate of 20 sccm. A typical ALD cycle consisted of a sequential and alternating supply of TTIP and H_2O as follows: a 0.5-s supply of TTIP vapor, a 3-s extended exposure of TTIP to GNSs, a 10-s N_2 purge, a 1-s supply of water vapor, a 3-s extended exposure of water vapor to

* Corresponding author. Tel.: +86 22 23766526; fax: +86 22 23766503.
E-mail addresses: xfli@mail.tjnu.edu.cn, xfli2011@hotmail.com (X. Li).

http://dx.doi.org/10.1016/j.elecom.2015.05.005
1388-2481/

GNSs, and another 10-s N_2 purge. The ALD processes were performed for 500 cycles at 100 °C to produce the amorphous TiO_2–GNS composites.

X-ray powder diffraction (XRD) patterns were collected on a Bruker D8 Discover Diffractometer using Co K_α radiation ($\lambda = 1.78897$ nm) at 40 kV and 100 mA. The morphologies and structures of amorphous TiO_2–GNSs were observed by a field emission scanning electron microscope (FE-SEM, Hitachi S-4800) and high-resolution transmission electron microscope (HRTEM, JEOL 2010 FEG). The thermogravimetric analysis (TGA) was performed on a TA SDT Q600 at air atmosphere from room temperature to 900 °C at a rate of 10 °C min^{-1}.

CR-2032-type coin cells were assembled in a glove box under a dry argon atmosphere. The working electrodes consist of 80 wt.% TiO_2–GNS composites as active material, 10 wt.% carbon black (M.M.M. Carbon, Belgium) as conductive agent and 10 wt.% poly(vinylidene) fluoride (Alfa Aesar) as binder. The introduction of 10 wt.% carbon black will help further increase the electrical conductivity of TiO_2 anode. The loading amount and density of the anode electrode are 3.2 mg cm^{-2} and 4.5 g cm^{-3}, respectively. The lithium foils (MTI Corp. USA) were used as the counter electrodes. The electrolyte (BASF) was composed of 1 M $LiPF_6$ salt dissolved in ethylene carbonate (EC):diethyl carbonate (DEC):ethyl methyl carbonate (EMC) of 1:1:1 volume ratio. The charge–discharge characteristics were galvanostatically tested between 1.0 and 3.0 V (vs. Li/Li^+) at room temperature using an Arbin BT-2000 Battery Tester.

3. Results and discussion

The morphologies and microstructures of the pristine GNSs and TiO_2–GNS composites were investigated by scanning electron microscopy (SEM). Fig. 1a shows the typical SEM images of the pristine GNSs. Obviously, GNSs tend to overlap and stick together into fluffy agglomerates with a worm-like appearance (see Fig. 1a inset). GNSs exhibit ultrathin, wrinkled and curved gossamer-like structure, as previously reported by our group [20,21]. In the case of the TiO_2–GNS composites (see Fig. 1b), the increased thickness of nanosheets indicates that a uniform amorphous TiO_2 thin film was homogenously deposited on both sides of GNSs via ALD. The resultant nanocomposites reveal a layer-by-layer assembled structure by TiO_2 particles with the sandwich-structured

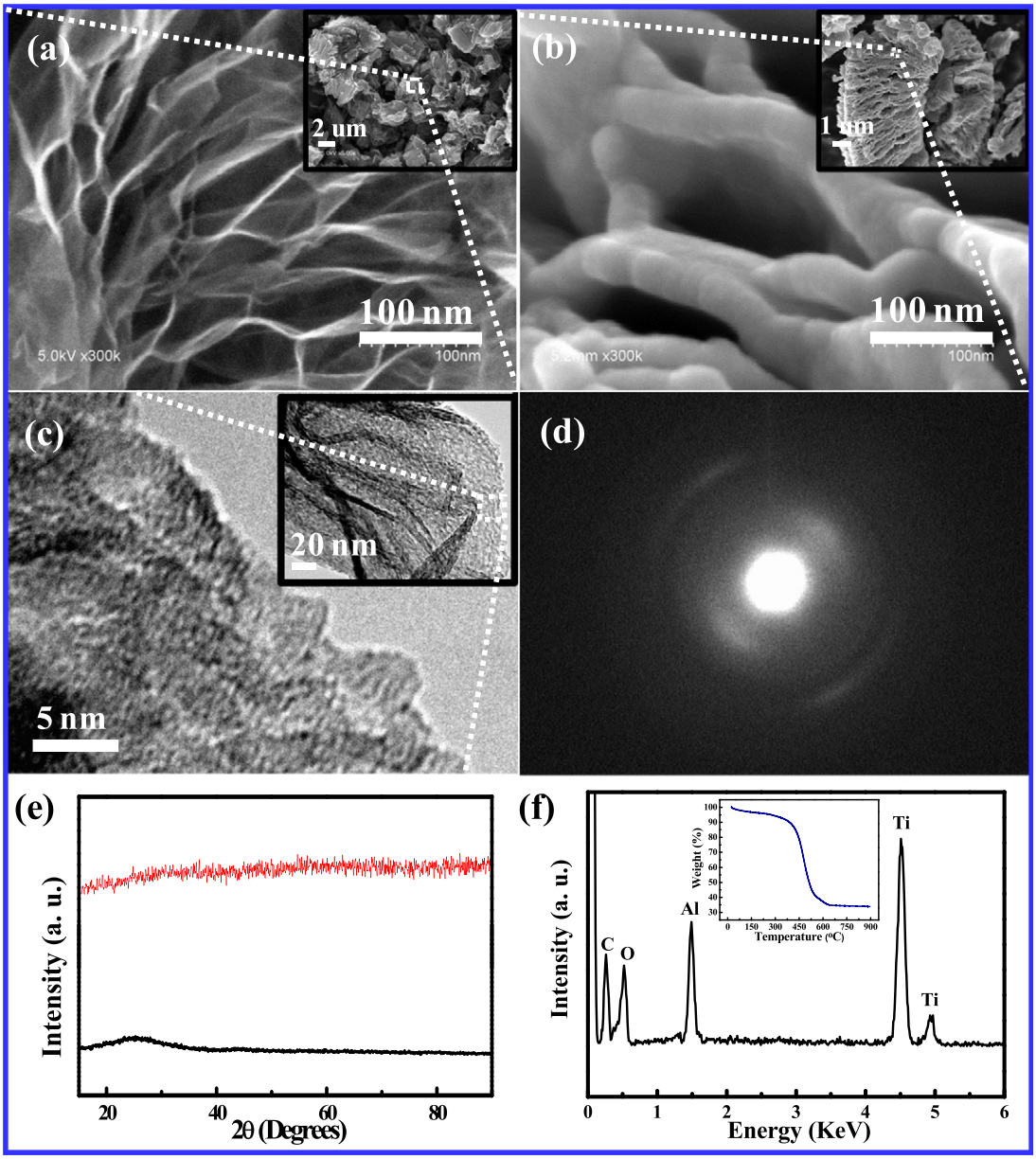

Fig. 1. Typical SEM images of (a) GNSs and (b) TiO_2–GNSs; (c) HRTEM, (d) Selective area electron diffraction (SAED), (e) XRD patterns, and (f) EDX spectra of TiO_2–GNSs (inset: TGA curve).

TiO_2–GNS composites. On basis of the mechanism of ALD process [16,17], the amorphous TiO_2 exhibits strong contact adhesion with 2D GNSs, and the designed nanocomposite significantly improves electrical conductivity of TiO_2. Fig. 1c shows a HRTEM image of the composites. No obvious lattice fringing of TiO_2 was observed, demonstrating successful deposition of amorphous TiO_2 on GNSs, which was further confirmed by the selective area electron diffraction (SAED) result with a diffused halo ring totally differing from crystalline rings (Fig. 1d).

The crystallinity degree of TiO_2 nanomaterials deposited on GNSs via ALD was determined by XRD. As shown in Fig. 1e, GNSs show a broad diffraction reflection observed at $2\theta = 26.8°$ with the extensive conjugated sp2 carbon network corresponding to the ordered crystal structure of graphite structure [22], while no reflections are observed in the TiO_2–GNS composites due to the presence of amorphous TiO_2, which is assigned to the absence of crystalline phases, originating from the synthesis conditions using ALD. As elucidated by our previous work [20], the growth temperature plays an important role in determining the degree of crystallinity of ALD derived nanomaterials. The deposition temperature employed in this study causes the formation of amorphous TiO_2 onto GNSs. The compositions of the TiO_2–GNS composites were further confirmed via EDX (see Fig. 1f). Various C, Ti, and O peaks were observed for the TiO_2–GNS composites (the peak of Al results from the Al sample holder). The thermogravimetric analysis (TGA) was carried out to measure TiO_2 loading on GNSs, as shown in Fig. 1f inset. It was found that the loading of TiO_2 is 49 wt.% in the nanocomposites.

The electrochemical behavior of TiO_2–GNS composites was evaluated by galvanostatic charge–discharge testing. Normally, the potential plateau confirms the equilibrium between lithium-rich and lithium-poor domains of crystalline anatase TiO_2 [23]. As shown in Fig. 2a, the TiO_2–GNS composites show a slope profile of voltage–capacity relationship for both charge and discharge, and no obvious plateau is observed, which reveals the absence of crystalline unlithiated and lithiated phases originating from the amorphous nature of deposited TiO_2 via ALD [24]. The first discharge and charge capacities of TiO_2–GNS composites were 200 and 150 mAh g^{-1}, respectively. The irreversible capacity of ~50 mAh g^{-1} was mainly ascribed to Li-ion insertion into irreversible sites and electrolyte decomposition [1–3,25]. In the subsequent cycles, the potential profiles of TiO_2-GNS composites almost overlap with excellent reversibility. Fig. 2b shows the cycle performance of the TiO_2–GNS composites at a specific current of 100 mA g^{-1}, and the amorphous TiO_2/GNS anode can deliver a reversible discharge capacity of

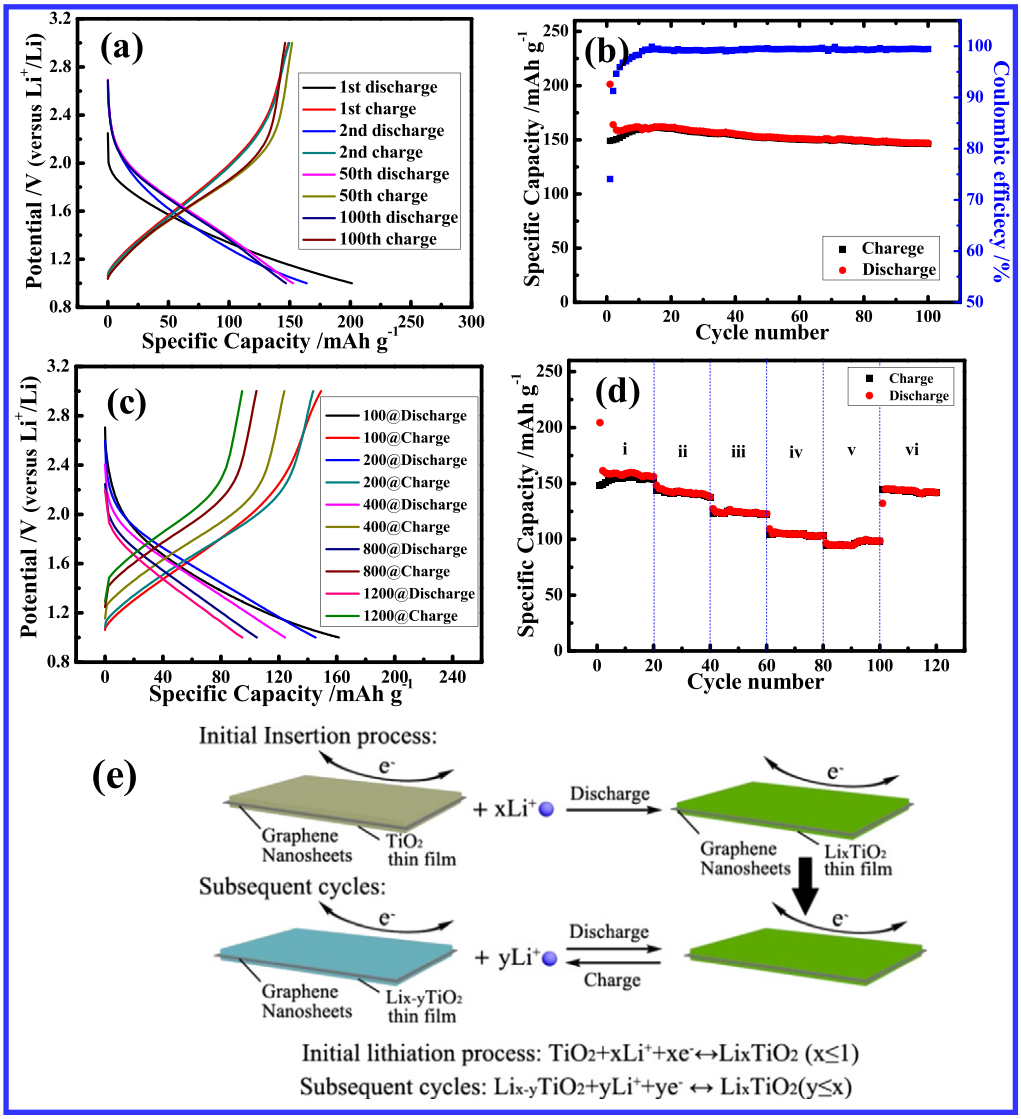

Fig. 2. (a) Charge/discharge profiles of TiO_2–GNSs at a specific current of 100 mA g^{-1}; (b) Reversible charge/discharge capacity and coulombic efficiency verse cycle number of TiO_2–GNSs at a specific current of 100 mA g^{-1}; (c) Charge/discharge profiles of TiO_2–GNSs at various specific currents; (d) Rate capability of TiO_2–GNSs at various specific currents: (i) 100, (ii) 200, (iii) 400, (iv) 800, (v) 1200, and (vi) 100 mA g^{-1}; and (e) Schematic illustration of electrochemical reaction mechanism of TiO_2–GNSs upon cycling.

140 mAh g^{-1} after 100 cycles with high capacity retention of 93.3% compared with the initial reversible capacity. This designed hybrid anode showed higher capacity retention than previously reported amorphous TiO_2 nanoparticles with a 50% capacity retention after 50 cycles [24], which highlights the importance of GNSs in the nanocomposites. Moreover, the Coulombic efficiency of the TiO_2–GNS composites approaches 100% after 10 cycles. The attractive cycle performance results from the amorphous TiO_2 nature as well as the synergistic effects of the TiO_2–GNS structure, large surface accessible to electrolyte of GNSs, short diffusion length of Li^+ and high electrical conductivity along porous GNSs.

To further demonstrate the advantages of amorphous TiO_2 based anode materials, the rate capability of the TiO_2–GNSs was tested. The samples were charged and discharged using various specific currents. As shown in Fig. 2c, the potential profiles at a higher specific current (eg. 1200 mA g^{-1}) almost maintain the similar slope shape compared with that of 100 mA g^{-1}, revealing excellent stability at higher rates. Fig. 2d displays the rate capability of the TiO_2–GNS composites, and the as-prepared nanocomposite anode delivers the reversible capacities of 150, 135, 125, 100 and 95 mAh g^{-1} at various specific currents of 100, 200, 400, 800 and 1200 mA g^{-1}, respectively. In particular, for a specific current of 100 mA g^{-1} after 100 cycles, the capacity of ~145 mAh g^{-1} is very close to the value of the 100th cycle in Fig. 2b, clearly demonstrating superior rate capability of TiO_2–GNS nanocomposites. One can see that the relative capacity retention at a specific current of 1200 mA g^{-1} is almost 60% compared with that of 100 mA g^{-1}, further confirming good rate capability of the TiO_2–GNS composites. At all specific currents, the specific capacities clearly decrease with increasing specific currents, which is a phenomenon typically observed in LIB electrodes. Normally, lithium ion diffusion within the TiO_2 anode slowly behaves, which dominates the process of lithium insertion. As a result, a lot of lithium ions accumulate on the interface of TiO_2 particles and electrolyte. In particular, the lithium ion motion across the interface and/or within the TiO_2 anode is slow for the charge distribution to obtain equilibrium at high specific current. Thus, with the increase of specific currents, the reversible capacity of the TiO_2 anode decreases [26,27].

As shown in Fig. 2e, Li_xTiO_2 could be formed upon lithium insertion in the initial discharge process. In subsequent process, lithium insertion/extraction of Li_xTiO_2 is reversible [24]. Upon cycling, the TiO_2 anode with volume change possibly leads to poor cycle performance mainly originating from destruction of conduction-pass-network in the electrode and low electrical conductivity. In this study, the electrochemical results reveal that the TiO_2–GNS composites exhibit good cycling performance and rate performance, which can be explained as follows: First, the wrinkled and curved gossamer-like GNSs with the amorphous nature of TiO_2 may significantly stabilize the volume change and possible pulverization of the anodes. Second, the amorphous TiO_2 anode shows intrinsically isotropic nature, which is benefical for increasing lithium diffusion into TiO_2. Third, as shown in Fig. 2e, the wrinkled and curved gossamer-like GNSs with high electrical conductivity overcome the TiO_2 disadvantage of low electrical conductivity, which facilitates lithium insertion/extraction kinetics [28,29]. Fourth, the uniform amorphous TiO_2 film reduces path length for Li-ion diffusion and benefits from activation process. Last, on basis of the strong adhesion of TiO_2 film with GNSs, the novel nanostructure can maintain the integrity and structural stability during the charge and discharge processes, responsible for high rate performance and cycling stability.

4. Conclusions

A composite of GNSs decorated with amorphous TiO_2 thin film was successfully synthesized via ALD. It was observed that the TiO_2 thin film was uniformly deposited onto GNSs. TiO_2–GNSs deliver a stable capacity of ~140 mAh g^{-1} at a specific current of 100 mA g^{-1} after 100 cycles. Moreover, the nanocomposites exhibit superior rate capability (95 mAh g^{-1} at 1200 mA g^{-1}). It is believed that the facile ALD approach will be a promising technique to increase TiO_2 anode performance for advanced energy-storage devices.

Acknowledgments

This research was supported by the Key Project of Tianjin Municipal Natural Science Foundation of China (14JCZDJC32200), the Open Project of Key Laboratory of Functional Inorganic Material Chemistry (Heilongjiang University), Ministry of Education, LPMT, CAEP (KF14006), and Academic Innovation Funding of Tianjin Normal University (52XC1404), and the program of Thousand Youth Talents in Tianjin of China.

References

[1] S. Brutti, V. Gentili, H. Menard, B. Scrosati, P.G. Bruce, TiO_2-(B) nanotubes as anodes for lithium batteries: origin and mitigation of irreversible capacity, Adv. Energy Mater. 2 (2012) 322–327.
[2] G. Zampardi, E. Ventosa, F.L. Mantiab, W. Schuhmann, In situ visualization of Li-ion intercalation and formation of the solid electrolyte interphase on TiO_2 based paste electrodes using scanning electrochemical microscopy, Chem. Commun. 49 (2013) 9347–9349.
[3] D. Bresser, E. Paillard, E. Binetti, S. Krueger, M. Striccoli, M. Winter, S. Passerini, Percolating networks of TiO_2 nanorods and carbon for high power lithium insertion electrodes, J. Power Sources 206 (2012) 301–309.
[4] Z.G. Yang, D. Choi, S. Kerisit, K.M. Rosso, D.H. Wang, J. Zhang, G. Graff, J. Liu, Nanostructures and lithium electrochemical reactivity of lithium titanites and titanium oxides: a review, J. Power Sources 192 (2009) 588–598.
[5] M.C. Kim, Y.W. Lee, S.J. Kim, B.M. Hwang, H.C. Park, E.T. Hwang, G.Z. Cao, K.W. Park, Improved lithium ion behavior properties of TiO_2@graphitic-like carbon core@shell nanostructure, Electrochim. Acta 147 (2014) 241–249.
[6] Z. Wang, J. Sha, E. Liu, C. He, C. Shi, J. Li, N. Zhao, A large ultrathin anatase TiO_2 nanosheet/reduced graphene oxide composite with enhanced lithium storage capability, J. Mater. Chem. A 2 (2014) 8893–8901.
[7] N. Li, G. Liu, C. Zhen, F. Li, L. Zhang, H. Cheng, Battery performance and photocatalytic activity of mesoporous anatase TiO_2 nanospheres/graphene composites by template-free self-assembly, Adv. Funct. Mater. 21 (2011) 1717–1722.
[8] G. Armstrong, A.R. Armstrong, P.G. Bruce, P. Reale, B. Scrosati, TiO_2(B) nanowires as an improved anode material for lithium-ion batteries containing $LiFePO_4$ or $LiNi_{0.5}Mn_{1.5}O_4$ cathodes and a polymer electrolyte, Adv. Mater. 18 (2006) 2597–2600.
[9] X. Yang, Y. Yang, H. Hou, Y. Zhang, L. Fang, J. Chen, X. Ji, Size-tunable single-crystalline anatase TiO_2 cubes as anode materials for lithium ion batteries, J. Phys. Chem. C 119 (2015) 3923–3930.
[10] Y. Yang, X. Ji, M. Jing, H. Hou, Y. Zhu, L. Fang, X. Yang, Q. Chen, C. Banks, Carbon dots supported upon N-doped TiO_2 nanorods applied into sodium and lithium ion batteries, J. Mater. Chem. A 3 (2015) 5648–5655.
[11] H. Fang, M. Liu, D. Wang, T. Sun, D. Guan, F. Li, J. Zhou, T. Sham, H. Cheng, Comparison of the rate capability of nanostructured amorphous and anatase TiO_2 for lithium insertion using anodic TiO_2 nanotube arrays, Nanotechnology 20 (2009) 225701.
[12] X. Zhang, P. Kumar, V. Aravindan, H. Liu, J. Sundaramurthy, S. Mhaisalkar, H. Duong, S. Ramakrishna, S. Madhavi, Electrospun TiO_2–graphene composite nanofibers as a highly durable insertion anode for lithium ion batteries, J. Phys. Chem. C 116 (2012) 14780–14788.
[13] K. Novoselov, A. Geim, S. Morozov, D. Jiang, Y. Zhang, S. Dubonos, I. Grigorieva, A. Firsov, Electric field effect in atomically thin carbon films, Science 306 (2004) 666–669.
[14] H. Wang, L. Cui, Y. Yang, H. Casalongue, J. Robinson, Y. Liang, Y. Cui, H. Dai, Mn_3O_4–graphene hybrid as a high-capacity anode material for lithium ion batteries, J. Am. Chem. Soc. 132 (2010) 13978–13980.
[15] S. Yu, L. Yang, Y. Tian, P. Yang, F. Jiang, S. Hu, X. Wei, J. Zhong, Mesoporous anatase TiO_2 submicrospheres embedded in self-assembled three-dimensional reduced graphene oxide networks for enhanced lithium storage, J. Mater. Chem. A 1 (2013) 12750–12758.
[16] C. Marichy, M. Bechelany, N. Pinna, Atomic layer deposition of nanostructured materials for energy and environmental applications, Adv. Mater. 24 (2012) 1017–1032.
[17] M. Knez, K. Niesch, L. Niinisto, Synthesis and surface engineering of complex nanostructures by atomic layer deposition, Adv. Mater. 19 (2007) 3425–3438.
[18] I.D. Scott, Y.S. Jung, A.S. Cavanagh, Y. Yan, A.C. Dillon, S.M. George, S.H. Lee, Ultrathin coatings on nano-$LiCoO_2$ for Li-ion vehicular applications, Nano Lett. 11 (2010) 414–418.
[19] Y.S. Jung, A.S. Cavanagh, L.A. Riley, S.H. Kang, A.C. Dillon, M.D. Groner, S.M. George, S.H. Lee, Ultrathin direct atomic layer deposition on composite electrodes for highly durable and safe Li-ion batteries, Adv. Mater. 22 (2010) 2172–2176.
[20] X. Li, X. Meng, J. Liu, D. Geng, Y. Zhang, M.N. Banis, Y. Li, J. Yang, R. Li, X. Sun, M. Cai, M.W. Verbrugge, Tin oxide with controlled morphology and crystallinity by atomic layer deposition onto graphene nanosheets for enhanced lithium storage, Adv. Funct. Mater. 22 (2012) 1647–1654.
[21] X. Li, Y. Hu, J. Liu, A. Lushington, R. Li, X. Sun, Structurally tailored graphene nanosheets as lithium ion battery anodes: an insight to yield exceptionally high lithium storage performance, Nanoscale 5 (2013) 12607–12615.

[22] E. Yoo, J. Kim, E. Hosono, H. Zhou, T. Kudo, I. Honma, Large reversible Li storage of graphene nanosheet families for use in rechargeable lithium ion batteries, Nano Lett. 8 (2008) 2277–2282.
[23] W.J.H. Borghols, M. Wagemaker, U. Lafont, E.M. Kelder, F.M. Mulder, Impact of nanosizing on lithiated rutile TiO_2, Chem. Mater. 20 (2008) 2949–2955.
[24] Y.M. Lin, P.R. Abel, D.W. Flaherty, J. Wu, K.J. Stevenson, A. Heller, C.B. Mullins, Morphology dependence of the lithium storage capability and rate performance of amorphous TiO_2 electrodes, J. Phys. Chem. C 115 (2011) 2585–2591.
[25] W.J.H. Borghols, D. Lutzenkirchen-Hecht, U. Haake, W. Chan, U. Lafont, E.M. Kelder, E.R.H. van Eck, A.P.M. Kentgens, F.M. Mulder, M. Wagemaker, Lithium storage in amorphous TiO_2 nanoparticles, J. Electrochem. Soc. 157 (2010) A582–A588.
[26] J.B. Goodenough, Y. Kim, Challenges for rechargeable Li batteries, Chem. Mater. 22 (2010) 587–603.
[27] K. Wang, X. Li, J. Chen, Surface and interface engineering of electrode materials for lithium-ion batteries, Adv. Mater. 27 (2015) 527–545.
[28] J. Jin, S. Huang, J. Liu, Y. Li, D. Chen, H. Wang, Y. Yu, L. Chen, B. Su, Design of new anode materials based on hierarchical, three dimensional ordered macro-mesoporous TiO_2 for high performance lithium ion batteries, J. Mater. Chem. A 2 (2014) 9699–9708.
[29] K. Xie, M. Guo, W. Lu, H. Huang, Aligned TiO_2 nanotube/nanoparticle heterostructures with enhanced electrochemical performance as three-dimensional anode for lithium-ion microbatteries, Nanotechnology 25 (2014) 455401.